ACS APPLIED MATERIALS & INTERFACES

www.acsami.org

Research Article

Novel Tunnel Magnetoresistive Sensor Functionalities via Oblique-Incidence Deposition

Svenja Willing,* Kai Schlage,* Lars Bocklage, Mohammad Mehdi Ramin Moayed, Tatiana Gurieva, Guido Meier, and Ralf Röhlsberger

Cite This: *ACS Appl. Mater. Interfaces* 2021, 13, 32343–32351

Read Online

ACCESS | Metrics & More | Article Recommendations

ABSTRACT: Controlling the magnetic properties of ultrathin films remains one of the main challenges to the further development of tunnel magnetoresistive (TMR) device applications. The magnetic response in such devices is mainly governed by extending the primary TMR trilayer with the use of suitable contact materials. The transfer of magnetic anisotropy to ferromagnetic electrodes consisting of CoFeB layers results in a field-dependent TMR response, which is determined by the magnetic properties of the CoFeB as well as the contact materials. We flexibly apply oblique-incidence deposition (OID) to introduce arbitrary intrinsic in-plane anisotropy profiles into the magnetic layers. The OID-induced anisotropy shapes the magnetic response and eliminates the requirement of additional magnetic contact materials. Functional control is achieved via an adjustable shape anisotropy that is selectively tailored for the ultrathin CoFeB layers. This approach circumvents previous limitations on TMR devices and allows for the design of new sensing functionalities, which can be precisely customized to a specific application, even in the high field regime. The resulting sensors maintain the typical TMR signal strength as well as a superb thermal stability of the tunnel junction, revealing a striking advantage in functional TMR design using anisotropic interfacial roughness.

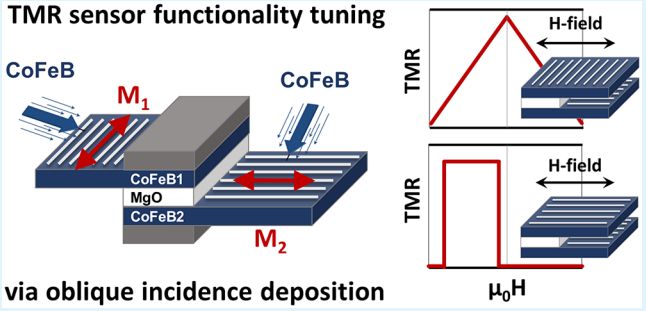

KEYWORDS: *magnetic field sensor, tunable sensor, tunnel magnetoresistance, oblique incidence deposition, interface morphology*

1. INTRODUCTION

Since the discovery of spin-dependent tunneling[1] and tunnel magnetoresistance[2,3] the race for ever increasing effect strengths of magnetic tunnel junctions (MTJs) has been ongoing.[4,5] A huge leap forward was made with the invention of grain-to-grain epitaxy in amorphous CoFeB layers annealed in contact with MgO. This approach combines the advantages of smooth amorphous materials with the spin-selective properties of epitaxial interfaces and a crystalline tunnel barrier.[6] Sensors based on the tunnel magnetoresistive (TMR) effect benefit from the resulting high effect strength exceeding 600% at room temperature.[7] In addition, such sensors can be small, are robust, provide contact-free measurement, and excel in energy efficiency due to an inherently large resistance. Hence, TMR sensors are widely used in a variety of different applications ranging from the detection of magnetic fields in the read heads of computer hard disk drives or e-compass hardware to electric current sensing and precision angle, position, and motion measurements in industrial robotics and especially automotive environments.

TMR sensors must satisfy a wide range of functionalities. In the case of magneto-cardiography applications, a given sensor must be capable of measuring the weak magnetic fields generated by the human heart.[8] Other applications require the capability to precisely sense the motions of an electromotor via detection of strong time-dependent stray magnetic fields. Thus, each TMR sensor needs to be adapted for its respective task. However, a lack of flexibility in their current functionality is the main limitation of conventional MTJs. In general, great effort is required to shape the sensor response. A given sensor is comprised of a number of sophisticated layer stacks which include various buffer layers as well as natural antiferromagnets. The latter ones are used for exchange-bias pinning of the magnetic reference layer and for the occasional soft pinning of the magnetic free layer.[9,10] Modifying a given stack design to a new magnetic field sensing range has proven to be quite challenging.

Here we use oblique-incidence deposition (OID)[11] to independently tailor the strength and orientation of the

Received: February 16, 2021
Accepted: June 15, 2021
Published: July 2, 2021

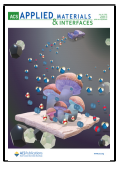

magnetic anisotropies in each of the CoFeB layers in a TMR stack to achieve three major advances. First, this method boosts the capabilities for new TMR functionality tuning and, second, allows for the unprecedented customization of the sensor functionality to the particular application. Moreover, it eliminates the need for an elaborate exchange-bias pinning for certain sensing tasks. Our approach combines the well-known CoFeB/MgO material system with the possibility to imprint a wide range of magnetic anisotropy profiles into the layer stack, hence opening new possibilities for the design and economic OID realization of TMR sensors with identical TMR layer building blocks.

1.1. Oblique Incidence Deposition of Magnetic Thin Films. OID or glancing angle deposition (GLAD) provides a convenient fabrication technique to drastically modify and precisely engineer thin-film properties for various applications like photonics, sensing, photovoltaics or batteries.[12,13] The basis for most OID applications are films with a thickness of more than 100 nm and a nanocolumnar structure that is initialized by atomic-scale shadowing during the deposition process.[14−16] The morphology of the growing nanocolumns can be flexibly designed and therefore functionalized via the sequence of deposition orientations relative to the film plane.

For magnetic films with a thickness of less than 20 nm, however, the nanoscopic origin of magnetic anisotropy shaping is different. In this early stage of OID growth, the high polar deposition angle ϑ between surface normal and particle flux results not yet in formation of a nanocolumnar film structure but in a continuous film with highly anisotropic surface roughness. A periodic wavy surface morphology with elongated islands can be identified in this case with wave fronts perpendicular to the deposition direction. The magnetic orientation of the films is oriented parallel to these wavefronts[17] (Figure 1).

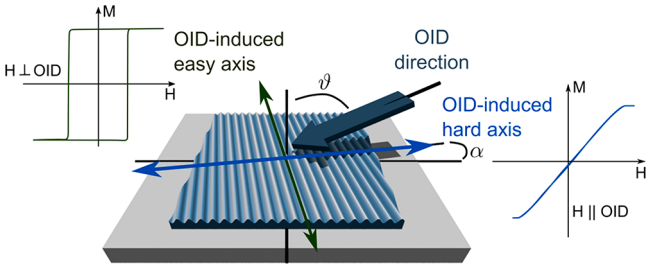

Figure 1. Oblique-incidence deposition of thin magnetic layers and induced magnetic anisotropy. The scheme displays the OID geometry as well as a simplified representation of developing anisotropic periodic surface roughness of the film and the corresponding induced shape anisotropy axes. Typical magnetic hysteresis curves for field sweeps perpendicular and parallel to the oblique-incidence direction are shown.

Via anisotropy calculations from measured surface morphologies of obliquely deposited iron thin films it was demonstrated that the origin of the resulting in-plane uniaxial magnetic anisotropy can be unambiguously attributed to the additional shape anisotropy and resulting long-range dipolar forces.[17] The anisotropy of these iron films increased continuously with increasing deposition angle ϑ reaching a maximum at around 80°. For a high deposition angle of 70°, the magnetic anisotropy likewise monotonously increased with increasing film thickness up to around 15 monolayers due to a build up in amplitude and wavelength of the correlated roughness.

The typical magnetic response of such an OID layer is no longer isotropic as shown in Figure 1. Magnetization measurements in an external field parallel to the wavefronts exhibit a sharp switching of the magnetization (left inset in Figure 1), while measurements with external fields parallel to the incidence direction reveal a rotation of the magnetization out of its easy axis (right inset in Figure 1). The polar deposition angle as well as the film thickness determine the strength of the shape anisotropy. Hence, material properties like coercive and saturation field can be widely tuned in single ferromagnetic layers and multilayer stacks enabling to realize easy axes switching fields of several tens of mT even with soft magnetic materials. In addition, the in-plane azimuthal deposition can be used to align the anisotropy axis for each individual layer. With this approach, the two angular degrees of freedom during deposition allow one to imprint arbitrary magnetic profiles into a multilayer stack.[11]

The combination of OID with the CoFeB/MgO system for TMR applications seems questionable at first glance. The as-sputtered CoFeB layers grow amorphously and only crystallize upon annealing. It is not *a priori* clear how the morphology-induced shape anisotropy can be combined with such a structural transition. A second challenge for OID-TMR systems is the ultrathin, high-quality, crystalline MgO tunnel barrier that has to be prepared on top of the wavy OID surface. We find that it is indeed possible to prepare magnetoresistive sensors of very high structural quality, based on the same TMR trilayer system with customized field responses by utilizing the anisotropy tuning offered via OID. Completely new sensor functionalities can be achieved, and novel sensor applications can be addressed by arbitrarily crossing the magnetization axes and setting the individual switching fields.

2. MATERIALS AND METHODS

The OID-TMR sensors discussed in the following have been prepared via magnetron sputter deposition onto naturally oxidized Si-wafer substrates. The sample holder can be positioned at arbitrary polar and azimuthal deposition angles with respect to the individual sputter source. TMR sensor stacks are as follows (thicknesses in nm): Si/SiO_2/Ta(5)/Ru(10)/Ta(5)/$CoFeB_{OID}$/MgO/$CoFeB_{OID}$/Ta(4)/Ru-(7), where the thicknesses of $Co_{20}Fe_{60}B_{20}$ and MgO as well as the respective polar deposition angles of CoFeB are given in the corresponding figures. Film preparation has been performed via standard direct current (dc) magnetron sputtering for all magnetic and metallic layers and radio frequency (rf) sputtering for the Si_3N_4 layer (see below). Information about relevant OID-related sputter deposition effects like the angular dependence of the deposition rate, characteristic OID film thickness gradients, and a convenient approach to prepare OID films with homogeneous thickness are given in ref 18.

The tunnel barrier was prepared either by radio frequency (rf) sputtering of a compound MgO target or, alternatively, of metallic Mg layers oxidized after deposition and capped with 0.3 nm of Mg. The latter barriers yielded higher TMR ratios (30−80%). The film samples were microstructured by laser lithography and ion-beam etching. The device design is shown in Figure 2. A buried bottom Ru electrode was used to connect the two sensors; the top contacts of each pair were contacted by Cr/Au pads on the Si_3N_4 insulation. The TMR stacks were structured to squares of about 20 μm edge length and annealed typically for 1 h at 350 °C either before or after microstructuring. Magnetic characterization was done via the longitudinal magneto-optical Kerr effect (MOKE). TMR was measured via dc two-point resistance measurements in a vector-magnet setup.

https://doi.org/10.1021/acsami.1c03084
ACS Appl. Mater. Interfaces 2021, 13, 32343−32351

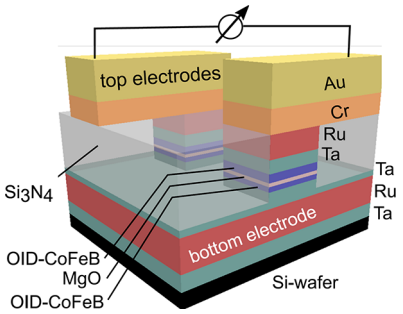

Figure 2. Device design of the microstructured OID-TMR sensors including obliquely deposited CoFeB as well as conventionally prepared MgO. The sensors are measured in pairs via their top contacts.

3. RESULTS

3.1. OID Anisotropy Tuning of Single CoFeB Thin Films. For the sensor functionalities, the anisotropy tuning in the CoFeB films is essential. We found that unlike for polycrystalline films the magnetic properties of the CoFeB layers depend on not only layer thickness and polar deposition angle but also the annealing temperature and contact material. The properties are governed by a sensitive balance of different anisotropy terms (magneto-elastic, magneto-crystalline, OID shape anisotropy, etc.). The predominance of the certain factors depends on various parameters. A detailed study on these dependencies can be found in ref 18 and a later publication.

The annealed and crystallized CoFeB layers exhibit an OID behavior with the easy axis of magnetization perpendicular to the OID direction as known from polycrystalline OID Fe or Co layers.[11,17] Figure 3a shows the magnetization curves obtained via MOKE of a series of 3 nm thick CoFeB single layers buffered and capped by 2 nm of Ta. The CoFeB layers have been prepared with different polar deposition angles and were annealed for 1 h at 300 °C for crystallization.

As can be seen from the slope of the curves and evolution of saturation fields, in this case OID also allows for the precise imprint of the strength of an associated uniaxial anisotropy and increases the thin film saturation fields in this usually soft-magnetic material. The data shown in Figure 3b are in agreement with the data for polycrystalline Fe films from refs 11 and 17.

Overall, OID can be used to widely adjust the magnetic hardness of annealed CoFeB thin films despite the corresponding amorphous−crystalline phase transition. Hence, OID paves the way to customizable TMR sensors as will be shown in section 3.3.

3.2. Interface Morphology. Information revealing the structural quality of the barrier region in a typical OID-TMR sensor environment was obtained via high-resolution transmission electron microscopy (HR-TEM), the results of which are shown in Figure 4. The MTJ in the imaged sample consists of two CoFeB layers prepared at high oblique incidence of 75 and 80° and a thickness of 2.5 and 3.0 nm separated by about 1.5 nm of MgO. The sample was annealed for 1 h at 350 °C prior to measurement. Figure 4a,b displays material-contrast measurements along two orthogonal directions. They confirm the wavy surface of the CoFeB layer with wavefronts perpendicular to the direction of incidence. The lateral correlation length of the OID-induced roughness along the azimuthal deposition direction (Figure 4b) is in the order of 8−10 nm. The same TEM image indicates a partial transfer of OID roughness from the lower magnetic electrode to the upper one, in which a significantly stronger granular surface morphology can be identified. Even for the upper CoFeB layer, the anisotropic roughness is only on the order of 2 nm.

The close-up of the MTJ in Figure 4c shows a high fraction of crystalline areas in the continued OID CoFeB layers as well as a partial crystalline order registering between MgO and CoFeB as desired in the grain-to-grain epitaxy process. Overall, from this and the later magnetoresistive measurements, it can be concluded that the quality of the tunnel barrier is not substantially affected by the OID-induced wavy morphology of the underlying CoFeB layer. This might be due to the fact that the OID surface profile has a wavelength which is nearly an order of magnitude larger than the barrier thickness. We found that even an MTJ with an ultrathin 9 Å MgO layer prepared from a compound target exhibits a sizable TMR signal.

A more pronounced OID morphology detectable with atomic force microscopy (AFM) of a $CoFeB_{75°}$/MgO/$CoFeB_{80°}$ trilayer system on a MgO buffer is shown in Figure 4d. The CoFeB layers are approximately 30% thicker compared to those shown in Figure 4a,b. The surface of this stack is characterized by an archetypal OID morphology with extended islands preferably orientated perpendicular to the azimuthal deposition orientation (black arrow). The height of the islands is now on the order of 4 nm and thus practically doubled, while the lateral correlation length also significantly

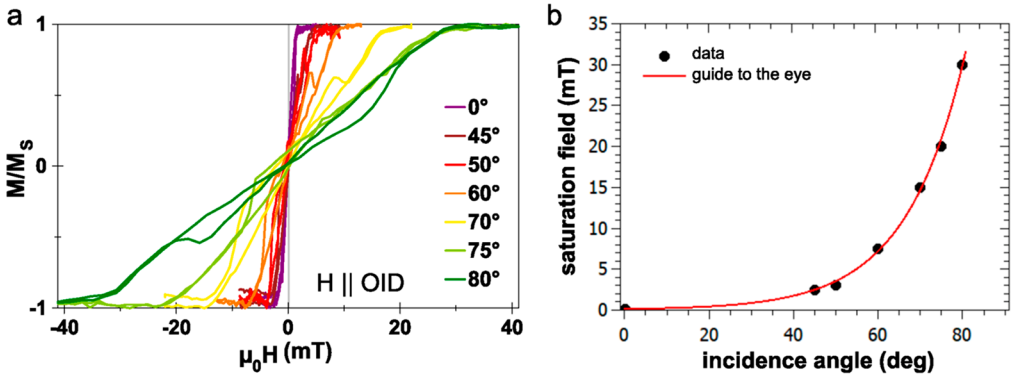

Figure 3. OID shape anisotropy tuning in annealed CoFeB single layers. (a) Hard axis MOKE measurements of annealed 3 nm thick CoFeB layers deposited at different oblique-incidence angles. (b) Extracted saturation field from Figure 3a as a function of polar deposition angle.

https://doi.org/10.1021/acsami.1c03084
ACS Appl. Mater. Interfaces 2021, 13, 32343−32351

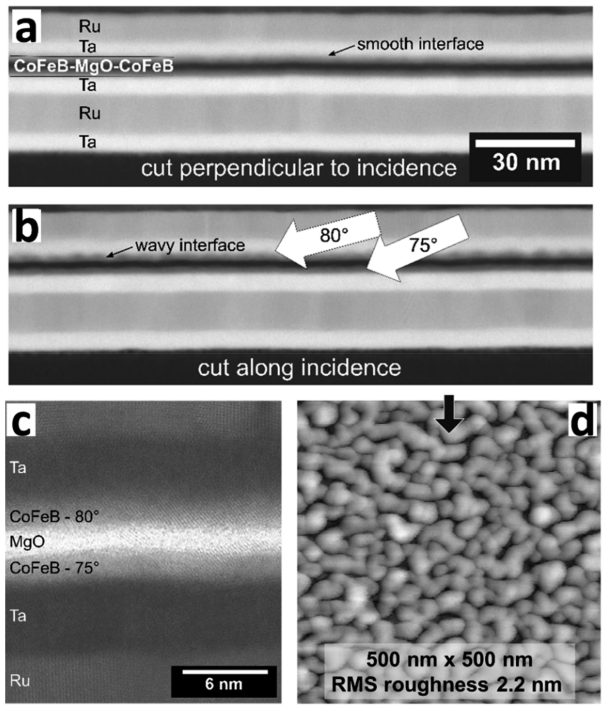

Figure 4. Magnetic tunnel junction after annealing with obliquely deposited CoFeB layers. (a, b) Material contrast high-resolution TEM images of an OID-TMR system with the indicated layer stack and an embedded CoFeB (2.5 nm, 75°)−MgO (1.5 nm)−CoFeB (3.0 nm, 80°) magnetic tunnel junction. The resulting wavy interface is only visible in the cut along the deposition incidence direction. (c) High-resolution TEM close-up of the annealed tunnel barrier region shows areas of matching crystalline structure in the obliquely deposited CoFeB and the MgO layer. (d) AFM image of an OID-TMR trilayer stack with thicker obliquly deposited magnetic electrodes on an MgO buffer and without capping. The black arrow depicts the azimutal deposition orientation of the upper CoFeB layer.

increased to about 25 nm. It should be mentioned that the typical CoFeB layer thicknesses for the TMR sensors discussed in the following are on the order of 1.5−3.0 nm.

3.3. Sensor Functionality Tuning. Figure 5 shows three exemplary OID-TMR sensor functionalities of microstructured devices. The first CoFeB/MgO/CoFeB trilayer is employed to yield a spin-valve-type TMR sensor response. The lower magnetic electrode (polar deposition angle 45°) acts in this case as sensing layer with a switching field close to remanence, while the upper one (80°) is used as reference magnetization. Both layers are prepared with an identical azimuthal deposition angle to realize parallel easy axes. We find that for field sweeps parallel to this axis the reversal of the magnetically softer electrode appears to be sharper compared to CoFeB layers deposited in normal incidence, most probably due to a more axial magnetic reversal and suppression of isotropic domain formation. For external field cycles with a maximal amplitude between 3 and 28 mT, only the lower electrode would reverse in this example, and the corresponding TMR signal will jump between a state of high resistance for the antiparallel magnetization state and a state of low resistance for the parallel magnetic configuration of both magnetic layers. The presented data set in Figure 5a shows the TMR signal for a full field sweep with a plateau of high resistance between the two different switching fields which can be flexibly adjusted via the parameters mentioned before.

If the two oblique depositions are chosen not to be parallel but with a finite relative azimuthal angle between them, then completely different functionalities can be achieved with the same trilayer structure. A 90° crossing of both easy axes, for instance, will result in a behavior that is interesting for many applications that require a linear sensor response practically without hysteresis. This can be achieved by an external field pointing along the hard axis of the magnetically harder CoFeB layer (see Figure 5b). The respective magnetization in the layer will rotate out of its easy axis leading to a linear response. If the other CoFeB layer is soft-magnetic and switches close to remanence, then the linear TMR function will invert upon field reversal resulting in the triangular shape seen in Figure 5b. This shape could be used for absolute field value measurements. In both cases, fine-tuning is possible via layer thicknesses and polar deposition angles to adjust the switching fields and the slope of the diagonal curve.

The OID-TMR stack introduced before can likewise be used to detect an in-plane rotary field as shown in Figure 5c. While the upper CoFeB layer is magnetically stabilized through a high polar deposition angle, the soft-magnetic lower layer is free to follow a small external rotary magnetic field and generates a sinusoidal response. This TMR stack can be used, for example, as an angle sensor.

3.4. Anisotropy Fine-Tuning in CoFeB/MgO/CoFeB Trilayers. To demonstrate the magnetic OID fine-tuning of a sensor response, we chose a TMR stack consisting of two OID-CoFeB layers. They exhibit parallel easy axes due to the same azimuthal deposition angle with a different strength of associated OID in-plane anisotropy due to different polar deposition angles. The MgO barrier thickness is approximately 1.5 nm.

An exemplary sample with high polar deposition angles of 75 and 80° has been annealed up to 1 h at 450 °C. It is lithographically structured only on one half to enable the comparison between MOKE-based magnetic measurements on the pristine film and magnetoresistive measurements of a structured device; see Figure 6a. As shown in Figure 5a, the magnetic field is swept along the layers' easy axes. While the TMR response displays the pronounced antiferromagnetic plateau of high resistance, a stepwise switching is seen in the MOKE measurements. Except for small variations in the absolute coercive field values due to the different measurement positions on opposite sides of the sample, both methods yield very comparable results. Hence, magnetic MOKE measurements of the film can give a good indication of a sensor's tunability. Furthermore, this simple double-switch sample reacts highly sensitive to variation of the deposition settings and therefore constitutes an ideal case to investigate the OID influence on the magnetic properties of the corresponding TMR sensors.

If one of the polar deposition angles of the OID-CoFeB layers is changed, then the respective coercive field varies accordingly. The MOKE curves in Figure 6b magnetically characterize TMR layer stacks in which the deposition angle of the upper CoFeB layer is increased from 65 to 80° which changes the associated switching field from about 1 to 3 mT. The absolute switching fields depend on the chosen OID sample stack, the CoFeB layer thickness, and in particular the annealing procedure. Here, the magnetically softer layer was prepared at 45° which, according to Figure 3b, barely leads to an additional OID shape anisotropy. The associated switching field remains constant at about 1 mT. The anisotropy of the

https://doi.org/10.1021/acsami.1c03084
ACS Appl. Mater. Interfaces 2021, 13, 32343−32351

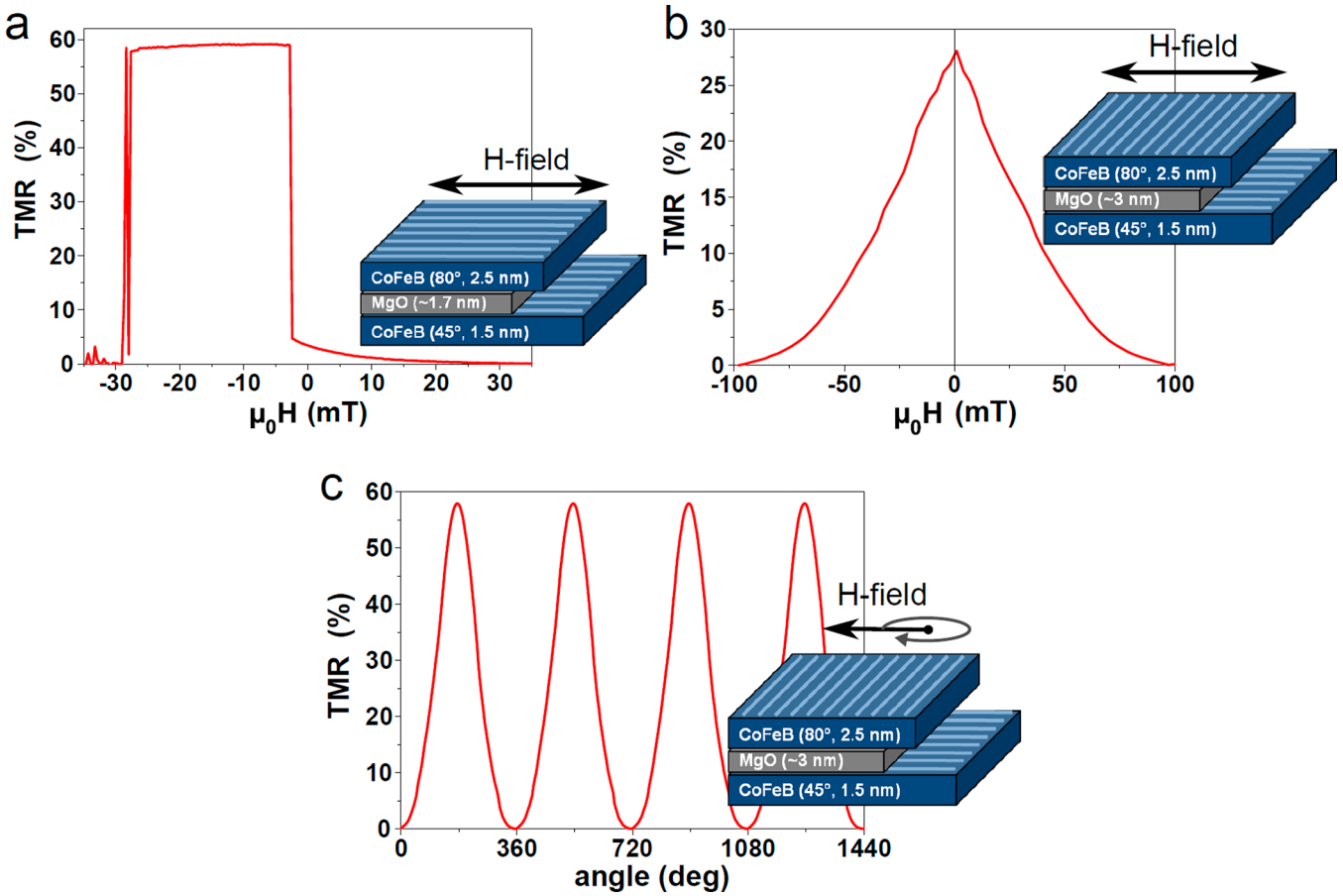

Figure 5. Multifunctional OID-TMR sensor. (a–c) TMR responses of $CoFeB_{OID}$/MgO/$CoFeB_{OID}$ junctions that were annealed for 1 h at 350 °C including sketches with the relevant OID parameters and external field directions. The lines on the CoFeB layers indicate the wavefronts due to oblique deposition. (a) Parallel easy axes result in the plateaulike spin-valve-type functionality. (b) A triangular absolute-value shape is achieved via a 90° crossing of the easy axes. (c) If the system from panel b is exposed to an in-plane rotary field, then the TMR response is approximately sinusoidal with a 360° periodicity.

upper CoFeB layer is individually adjustable because the waviness of the lower CoFeB layer is less than 1 nm.

However, for TMR systems with ultrathin tunnel barriers, both layers are not always separately tunable via OID: The wavy surface of the lower CoFeB layer can be partially transferred to the top layer via correlated roughness. Thus, both CoFeB layers could be rendered magnetically harder if the 45° layer below the tunnel barrier could be deposited more obliquely. As an example, Figure 6c shows MOKE data from three similar samples with varying polar deposition angle of the bottom CoFeB layer. Here, not only the switching field but also the plateau width is affected by the changes in deposition parameters. The effect of correlated roughness has to be kept in mind if the polar deposition angle of the bottom CoFeB layer is changed. It can be partially compensated by choosing the appropriately reduced deposition angle for the upper ferromagnetic layer.

Besides the angles, the magnetic layer thickness can also be used to increase the wavy OID profile and, hence, the coercivity and the plateau width of the sensor. In Figure 6d, the coercive fields of a gradient sample are summarized as a function of the CoFeB layer thicknesses. Both OID layers have a thickness gradient that changes the respective magnetic hardness. The behavior of this sample with ultrathin MgO spacer layer can be categorized in three regimes. At the thin regime I, the OID switching fields are low and similar, and a small dipolar interlayer coupling can cause a common switch during magnetic reversal. In regime II, the typical increase in OID-induced switching field strength with growing thickness[17] can be recognized for both layers. Because the top layer exhibits a stronger thickness gradient in this case due to preparation conditions, the increase in switching field is more pronounced. After a certain maximum around a thickness of 2.6 nm of the top layer, the width of the plateau decreases: In regime III, the wavy interface profile further increases with increasing layer thicknesses. This probably introduces a Néel[19] or orange peel coupling which favors a parallel alignment of magnetizations. Thus, with growing thickness and coupling, the two CoFeB layers increasingly act as one layer until there is only a single switch left. For TMR sensors with two parallel easy axes, the coercive fields and plateau region width can thus be tuned via the polar angles as well as the CoFeB layer thickness. According to ref 20, no significant effect of the magnetic layer thickness on the TMR effect strength was found. Hence, this enables advanced control of the switching fields and allows for customization of the TMR sensor to the requirements of a certain application.

3.5. Thermal Annealing. Unlike in material systems using Fe or Co that exhibit a polycrystalline structure as sputtered, the CoFeB layers grow, as mentioned before, amorphously and only crystallize upon annealing. Hence, the annealing process strongly defines magnetic and magnetoresistive properties via

https://doi.org/10.1021/acsami.1c03084
ACS Appl. Mater. Interfaces 2021, 13, 32343–32351

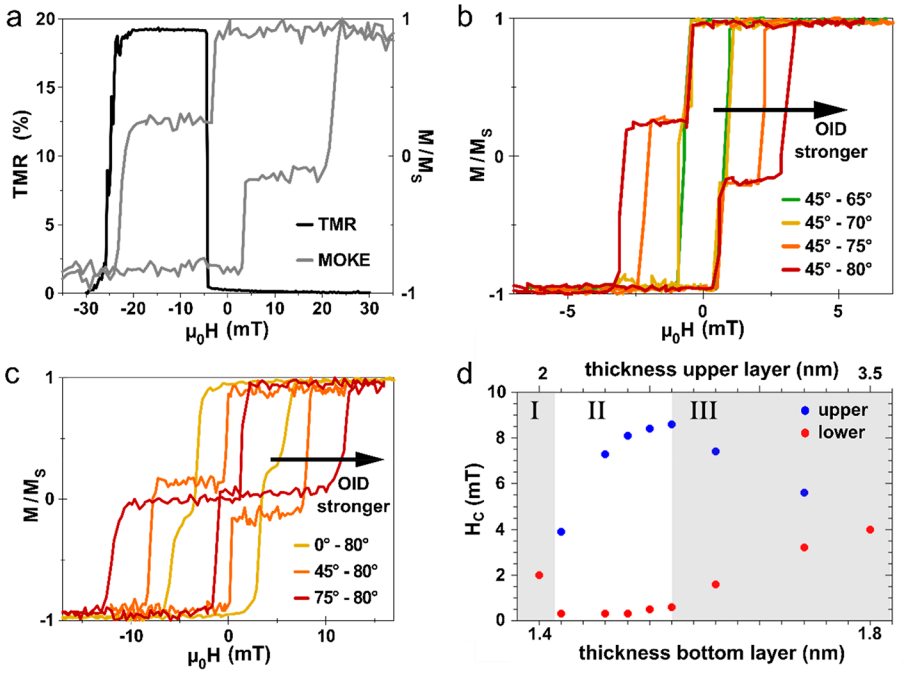

Figure 6. Tuning of magnetic response in a TMR layer system via variation of OID parameters. (a) Comparison of magnetic (MOKE) and magnetoresistive (TMR) measurements from an annealed stack structure identical to the one in Figure 4a. The lower and upper CoFeB layers have been deposited at 75 and 80°, respectively. (b, c) MOKE measurements of annealed sensors stacks similar to the one in Figure 4a. Only the polar deposition angles of the upper (b) or lower (c) CoFeB layer are varied as given in the respective key. (d) Coercive field values versus CoFeB layer thickness. Measurements are taken with a sample structure from Figure 4a, but with a thickness gradient in both CoFeB layers to investigate the influence of the OID material thickness on the magnetic properties.

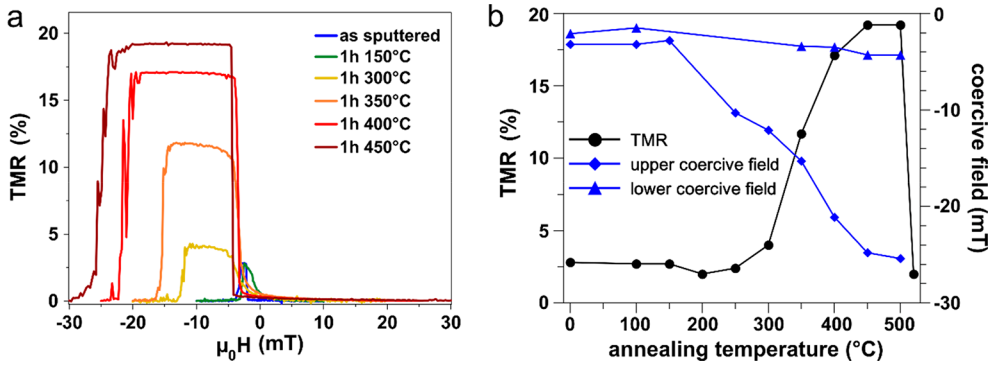

Figure 7. Influence of annealing temperature on magnetic and magnetoresistive properties. (a) TMR measurements of an OID-TMR sensor with polar deposition angles of 75 and 80° and parallel easy axes (layer structure identical to Figure 2). The data were taken using the same microstructured device after subsequent annealing steps with increasing temperature. (b) Evaluation of TMR effect strength, coercive fields and plateau width depending on annealing temperature of the data sets in (a).

the degree of polycrystallinity. The extend of this effect is summarized in Figure 7 where an increase in annealing temperature leads to higher absolute coercive field values, more pronounced switching behavior and an overall higher TMR effect. The changes in magnetic and magnetoresistive properties that accompany the structural transition were found to already start at around 200 °C below the typically expected crystallization temperature of around 300−350 °C.[18] This enhanced crystallization behavior was found in many OID CoFeB layers, confirmed by X-ray scattering techniques, and is assumed to be due to an improved Boron diffusion.[9] Surprisingly, the OID-induced wavy surface morphology seems to be stable up to high temperatures in the range of 500 °C making the OID-TMR sensors extremly robust.

3.6. OID Sensors with Exchange-Bias Pinning. Thus far, we have shown that OID allows for the preparation of fully functional and customized trilayers without additional magnetic contact materials in order to shape the TMR response. If the strength of accessible OID anisotropy for a reference magnetization within the trilayer (see Figure 5a,c) is not sufficient for certain high field applications, then the stack design can likewise be supplemented with additional pinning layers. As an exemplary demonstration, we combine the OID trilayer design of Figure 5b with a 90° crossing of the easy axes resulting in a triangular-shaped TMR response with an additional pinning layer substructure (Figure 8a) that is currently applied in conventional spin-valve-type systems.[21] This substructure magnetically pins the former soft-magnetic bottom CoFeB layer up to an external field strength of about

https://doi.org/10.1021/acsami.1c03084
ACS Appl. Mater. Interfaces 2021, 13, 32343−32351

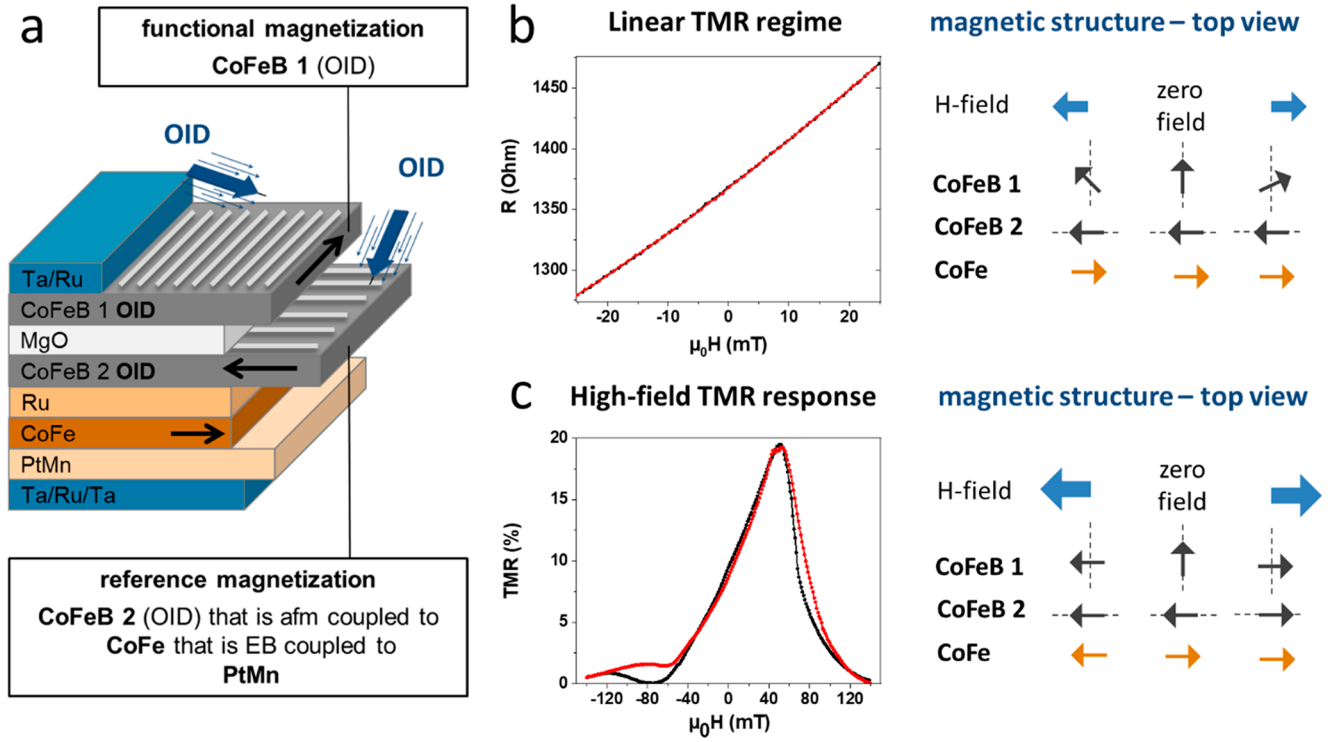

Figure 8. Linear TMR sensor response in an OID-system with additional magnetic pinning. (a) Sketch of the layer structure. An OID-TMR stack identical to that in Figure 5b is extended by a conventional pinning approach with a CoFe layer that is exchange coupled to a PtMn layer. This CoFe reference magnetization is transferred and strengthened via an antiferromagnetic Ru interlayer coupling to the lower CoFeB layer in the OID-TMR stack. (b) Low field TMR response and magnetic structure. Due to the pinning only the magnetization of the upper CoFeB is deflected by an external magnetic field leading to a linear TMR response for magnetic field sweeps along its hard OID axis. The field range of this reversible behavior is defined by the OID parameters of the top CoFeB layer and the stability of reference magnetization in the lower one. (c) TMR response and corresponding magnetic stack structure in the high field regime. The decrease in the magnetoresistance above +50 mT is due to a magnetic reorientation in the CoFe/Ru/CoFeB substructure. The bulge at around −100 mT is induced by a magnetic reorientation of the exchange-bias coupled CoFe layer on the antiferromagnetic PtMn.

100 mT and transforms the OID-TMR response now into an almost linear and hysteresis-free signal over a technically relevant field regime of ±25 mT (Figure 8b).

In this example, a 2.5 nm thick CoFe layer is exchange-coupled[21,22] to a 15 nm thick antiferromagnetic PtMn layer to realize a strong unidirectional reference magnetization. This stabilized magnetization direction is reversely transferred to the lower OID-CoFeB layer of the TMR stack via a strong antiferromagnetic interlayer coupling using a 0.9 nm thin Ru spacer layer.[23] This stack design additionally integrates the lower CoFeB layer into a closed magnetization loop with the CoFe layer of the substructure hence minimizing the stray fields of the lower CoFeB layer acting on the top OID-CoFeB layer. As a result, the top OID-CoFeB layer will "freely" respond to an external field sweep, rotate reversibly out of its easy axis, and produce a linear TMR signal. The magnetic saturation behavior and linear TMR response of the top CoFeB layer can be adjusted via the OID parameters in a field range of 0 to 100 mT. However, magnetic reorientation in the pinning substructure at high fields will directly modify the linearity of the TMR response (see Figure 8c).

Overall, this sensor as well as the ones shown in Figure 5 exhibit diverse and versatile TMR functionalities realized in practically the same layer system, simply using variations in the deposition direction of the magnetic material. The OID sensor functionalities exemplarily presented here can be further tailored and adjusted to the respective application via fine-tuning of the polar and azimuthal deposition angles. Through insertion of additional MgO/CoFeB$_{OID}$ double layers, the portfolio of possible TMR sensor functionalities could be further expanded, including flexible multiplateau characteristics with adjustable slopes and switching fields.

4. CONCLUSIONS

The oblique-incidence deposition of CoFeB layers in TMR stacks significantly advance their functionality. We have shown that the additional shape anisotropy induced via OID enables tuning of the magnetic properties of annealed CoFeB layers. Thus, the coercivity and direction of the magnetization axis in every ferromagnetic layer of a TMR sensor can be freely chosen through proper selection of both OID deposition angles (polar and azimuthal) and layer thickness. The OID thin films are in particular characterized by sharp magnetic switching fields. Moreover, hysteresis curves indicate domain-free remanent states. It was shown that it is possible to fabricate, measure, and tune magnetic tunnel junctions with obliquely deposited CoFeB layers that are characterized by a nanoscale wavy surface profile and separated by an ultrathin MgO tunnel barrier. These magnetically tailored TMR systems in MTJs have been successfully applied to achieve defined and adjustable double switch, triangular, linear, or sinusoidal TMR responses with almost the same material stack. An OID-TMR effect strength of up to 80% was accomplished so far and can probably be improved further by standard optimization routines like annealing and oxidation procedure of the barrier. The OID-approach and the CoFeB/MgO material system

https://doi.org/10.1021/acsami.1c03084
ACS Appl. Mater. Interfaces 2021, 13, 32343−32351

enable unique magnetic and TMR functionalities while keeping the high signal performance, excellent temperature stability, and good compatibility of common fabrication and microstructuring methods. OID thus offers an elegant route to significantly broaden the application spectrum of high-performance TMR sensors in a highly accessible and economic manner.

AUTHOR INFORMATION

Corresponding Authors

Kai Schlage − *Deutsches Elektronen-Synchrotron DESY, 22607 Hamburg, Germany;* orcid.org/0000-0002-5787-0037; Email: kai.schlage@desy.de

Svenja Willing − *Deutsches Elektronen-Synchrotron DESY, 22607 Hamburg, Germany; PIER Helmholtz Graduate School, 22607 Hamburg, Germany*; Email: sw@drwilling.de

Authors

Lars Bocklage − *Deutsches Elektronen-Synchrotron DESY, 22607 Hamburg, Germany; The Hamburg Centre for Ultrafast Imaging, 22761 Hamburg, Germany*

Mohammad Mehdi Ramin Moayed − *Deutsches Elektronen-Synchrotron DESY, 22607 Hamburg, Germany*

Tatiana Gurieva − *Deutsches Elektronen-Synchrotron DESY, 22607 Hamburg, Germany; Institut für Optik und Quantenelektronik, Friedrich-Schiller-Universität Jena, 07743 Jena, Germany; Helmholtz-Institut Jena, 07743 Jena, Germany*

Guido Meier − *The Hamburg Centre for Ultrafast Imaging, 22761 Hamburg, Germany; Max-Planck Institute for the Structure and Dynamics of Matter, 22761 Hamburg, Germany*

Ralf Röhlsberger − *Deutsches Elektronen-Synchrotron DESY, 22607 Hamburg, Germany; Institut für Optik und Quantenelektronik, Friedrich-Schiller-Universität Jena, 07743 Jena, Germany; Helmholtz-Institut Jena, 07743 Jena, Germany; Helmholtz Centre for Heavy Ion Research (GSI), 64291 Darmstadt, Germany*

Complete contact information is available at: https://pubs.acs.org/10.1021/acsami.1c03084

Notes

The authors declare no competing financial interest.

ACKNOWLEDGMENTS

We thank Meredith Henstridge for proofreading the manuscript and Andrey Siemens for technical support. We acknowledge support of the Helmholtz Association through project-oriented funds and by the Partnership for Innovation, Education and Research (PIER) between DESY and the University of Hamburg. This work is supported/funded by the Cluster of Excellence "CUI: Advanced Imaging of Matter" of the Deutsche Forschungsgemeinschaft (DFG) (EXC 2056, project ID 390715994).

REFERENCES

(1) Julliere, M. Tunneling between ferromagnetic films. *Phys. Lett. A* **1975**, *54A*, 225−226.

(2) Miyazaki, T.; Tezuka, N. Giant magnetic tunneling effect in Fe/Al_2O_3/Fe junction. *J. Magn. Magn. Mater.* **1995**, *139*, L231−L234.

(3) Moodera, J. S.; Kinder, L. R.; Wong, T. M.; Meservey, R. Large Magnetoresistance at Room Temperature in Ferromagnetic Thin Film Tunnel Junctions. *Phys. Rev. Lett.* **1995**, *74*, 3273−3276.

(4) Faure-Vincent, J.; Tiusan, C.; Jouguelet, E.; Canet, F.; Sajieddine, M.; Bellouard, C.; Popova, E.; Hehn, M.; Montaigne, F.; Schuhl, A. High tunnel magnetoresistance in epitaxial Fe/MgO/Fe tunnel junctions. *Appl. Phys. Lett.* **2003**, *82*, 4507.

(5) Parkin, S. S. P.; Kaiser, C.; Panchula, A.; Rice, P. M.; Hughes, B.; Samant, M.; Yang, S. Giant tunnelling magnetoresistance at room temperature with MgO (100) tunnel barriers. *Nat. Mater.* **2004**, *3*, 862.

(6) Djayaprawira, D. D.; Tsunekawa, K.; Nagai, M.; Maehara, H.; Yamagata, S.; Watanabe, N.; Yuasa, S.; Suzuki, Y.; Ando, K. 230% room-temperature magnetoresistance in CoFeB/MgO/CoFeB magnetic tunnel junctions. *Appl. Phys. Lett.* **2005**, *86*, No. 092502.

(7) Ikeda, S.; Hayakawa, J.; Ashizawa, Y.; Lee, Y. M.; Miura, K.; Hasegawa, H.; Tsunoda, M.; Matsukura, F.; Ohno, H. Tunnel magnetoresistance of 604% at 300 K by suppression of Ta diffusion in CoFeB/MgO/CoFeB pseudo-spin-valves annealed at high temperature. *Appl. Phys. Lett.* **2008**, *93*, No. 082508.

(8) Fujiwara, K.; Oogane, M.; Kanno, A.; Imada, M.; Jono, J.; Terauchi, T.; Okuno, T.; Aritomi, Y.; Morikawa, M.; Tsuchida, M.; et al. Magnetocardiography and magnetoencephalography measurements at room temperature using tunnel magneto-resistance sensors. *Appl. Phys. Express* **2018**, *11*, No. 023001.

(9) Negulescu, B.; Lacour, D.; Montaigne, F.; Gerken, A.; Paul, J.; Spetter, V.; Marien, J.; Duret, C.; Hehn, M. Wide range and tunable linear magnetic tunnel junction sensor using two exchange pinned electrodes. *Appl. Phys. Lett.* **2009**, *95*, 112502.

(10) Yuan, Z. H.; Huang, L.; Feng, J. F.; Wen, Z. C.; Li, D. L.; Han, X. F.; Nakano, T.; Yu, T.; Naganuma, H. Double-pinned magnetic tunnel junction sensors with spin-valve-like sensing layers. *J. Appl. Phys.* **2015**, *118*, No. 053904.

(11) Schlage, K.; Bocklage, L.; Erb, D.; Comfort, J.; Wille, H.-C.; Röhlsberger, R. Spin-Structured Multilayers: A New Class of Materials for Precision Spintronics. *Adv. Funct. Mater.* **2016**, *26*, 7423−7430.

(12) Hawkeye, M. M.; Taschuk, M. T.; Brett, M. J. *Glancing Angle Deposition of Thin Films - Engineering the Nanoscale*; Wiley Series in Materials for Electronic & Optoelectronic Applications; Wiley, 2014.

(13) Barranco, A.; Borras, A.; Gonzalez-Elipe, A. R.; Palmero, A. Gonzales-Elipe, Augustin R.; Palmero, A. Perspectives on oblique angle deposition of thin films: From fundamentals to devices. *Prog. Mater. Sci.* **2016**, *76*, 59−153.

(14) Abelmann, L.; Lodder, C. Oblique evaporation and surface diffusion. *Thin Solid Films* **1997**, *305*, 1−21.

(15) Robbie, K.; Brett, M. J. Sculptured thin films and glancing angle deposition: growth mechanics and applications. *J. Vac. Sci. Technol., A* **1997**, *15*, 1460−1465.

(16) Tao, Y.; Degen, C. L. Growth of magnetic nanowires along freely selectable ⟨*hkl*⟩ crystal directions. *Nat. Commun.* **2018**, *9*, 339.

(17) Bubendorff, J. L.; Zabrocki, S.; Garreau, G.; Hajjar, S.; Jaafar, R.; Berling, D.; Mehdaoui, A.; Pirri, C.; Gewinner, G. Origin of the magnetic anisotropy in ferromagnetic layers deposited at oblique incidence. *Europhys. Lett.* **2006**, *75*, 119−125.

(18) Willing, S. Oblique-incidence deposition of ferromagnetic thin films and their application in magnetoresistive sensors. Dissertation, University of Hamburg, 2020.

(19) Néel, L. Sur un nouveau mode de couplage entre les animantations de deux couches minces ferromagnetiques. *C. R. Acad. Sci.* **1962**, *255*, 1676.

(20) Parkin, S. S. P.; Kaiser, C.; Panchula, A.; Rice, P. M.; Hughes, B.; Samant, M.; Yang, S.-H. Giant tunnelling magnetoresistance at room temperature with MgO (100) tunnel barriers. *Nat. Mater.* **2004**, *3*, 862−867.

(21) Lee, Y. M.; Hayakawa, J.; Ikeda, S.; Matsukura, F.; Ohno, H. Giant tunnel magnetoresistance and high annealing stability in CoFeB/MgO/CoFeB magnetic tunnel junctions with synthetic pinned layer. *Appl. Phys. Lett.* **2006**, *89*, No. 042506.

(22) Nogués, J.; Schuller, I. K. Exchange bias. *J. Magn. Magn. Mater.* **1999**, *192*, 203−232.

(23) Wiese, N.; Dimopoulos, T.; Rührig, M.; Wecker, J.; Brückl, H.; Reiss, G. Antiferromagnetically coupled CoFeB/Ru/CoFeB trilayers. *Appl. Phys. Lett.* **2004**, *85*, 2020.

https://doi.org/10.1021/acsami.1c03084
ACS Appl. Mater. Interfaces 2021, 13, 32343−32351